

VO_x/SiO₂ Catalyst Prepared by Grafting VOCl₃ on Silica for Oxidative Dehydrogenation of Propane

Haibo Zhu,^[a] Samy Ould-Chikh,^[a] Hailin Dong,^[a] Isabelle Llorens,^[b] Youssef Saih,^[a] Dalaver H. Anjum,^[c] Jean-Louis Hazemann,^[d] and Jean-Marie Basset*^[a]

The VO_x/SiO₂ catalysts for oxidative dehydrogenation of propane were synthesized by a simple grafting method. The VOCl₃ was first grafted at the surface of SiO₂, which was dehydrated at different temperature (from 200 to 1000 °C). The formed grafted complexes were then calcined in air, leading to the formation of VO_x/SiO₂ catalysts. The synthesized catalysts were characterized by nitrogen adsorption, SEM, Raman spectroscopy, temperature-programmed reduction, and extended X-ray absorption fine structure analysis. The SiO₂ pretreatment

temperature has an evident effect on the loading and dispersion of VO_x on SiO₂, which finally affects their catalytic performance. High SiO₂ treatment temperature is beneficial to dispersing the vanadium oxide species at the SiO₂ surface. These materials are efficient catalysts for the catalytic oxidative dehydrogenation of propane to propylene. The best selectivity to propylene is achieved on the VO_x/SiO₂₋₍₁₀₀₀₎ catalyst. The high selectivity and activity are well maintained for three days catalytic reaction.

Introduction

Propylene is a major industrial chemical intermediate. It is used as the basic building blocks for an array of chemicals and plastics production, such as polypropylene, acrylic acid, and acetone. The global propylene market increases each year owing to a large consumption of the downstream products derived from propylene. Therefore, much research efforts have been dedicated to the development of new technologies or processes for the efficient production of propylene all over the world.^[1]

Nowadays propylene is produced from the feedstock of crude oil and natural gas by steam cracking, fluid catalytic-cracking, and catalytic dehydrogenation processes.^[1a,2] The development of a less energy-intensive process for the propylene production would be advantageous compared with these traditional processes. The thermodynamically favored oxidative dehydrogenation (ODH) of propane is an attractive alternative

process for the existing propylene production.^[1b] A great variety of catalysts with various compositions have been used in the production of propylene from propane by ODH.^[3] Among these catalysts, the vanadia dispersed on different "classical" supports, such as SiO₂, Al₂O₃, TiO₂, and ZrO₂, has been found to be the most active catalyst for the propane ODH reaction.^[4] Indeed, this kind of supported vanadia catalyst is proven to be a structure-sensitive catalyst, and its catalytic performance is closely related to the dispersion of vanadium oxide at the surface of support.^[4a]

It has been demonstrated that the preparation method has a significant influence on the nature of VO_x species at the surface of the support. To develop effective vanadia catalyst for propane ODH, a variety of synthetic methods, such as impregnation,^[5] grafting,^[6] thermolytic molecular precursor,^[7] atomic layer deposition,^[8] and flame spray pyrolysis,^[9] have been applied. Herein, we use a grafting method to anchor VOCl₃ at the surface of SiO₂. The density of grafting sites (OH groups) at the silica surface is strongly dependent on its dehydroxylation temperature, and thus the final VO_x loading and dispersion at SiO₂ surface can be controlled systematically by the variation of SiO₂ pretreatment temperature. The produced VO_x/SiO₂ catalysts exhibit different level of activity and selectivity in propane ODH reaction.

Results and Discussion

Characterization of catalysts

It is well known that the density and structure of OH group at the surface of SiO₂ is sensitive to its treatment temperature.^[10] If the SiO₂ is calcined at different temperatures, dehydration, dehydroxylation, and rehydroxylation processes will occur at

[a] Dr. H. Zhu, Dr. S. Ould-Chikh, Dr. H. Dong, Dr. Y. Saih, Prof. J.-M. Basset
KAUST Catalysis Center
King Abdullah University of Science and Technology
Thuwal 23955-6900 (Kingdom of Saudi Arabia)
E-mail: Jeanmarie.basset@kaust.edu.sa

[b] Dr. I. Llorens
Institut de Recherches sur la Catalyse et l'Environnement de Lyon
IRCELYON, UMR 5256
CNRS—Université Lyon 1
2 av. A. Einstein, 69626 Villeurbanne Cedex (France)

[c] Dr. D. H. Anjum
KAUST Core Lab
King Abdullah University of Science and Technology
Thuwal 23955-6900 (Kingdom of Saudi Arabia)

[d] Dr. J.-L. Hazemann
Institut Neel, CNRS
25, avenue des Martyrs, F-38042 Grenoble Cedex 9 (France)

Supporting Information for this article is available on the WWW under <http://dx.doi.org/10.1002/cctc.201500607>.

the surface of SiO₂, which leads to the reconstruction of the surface and, in particular, the nature of silanol groups and ≡Si–O–Si≡ moieties. Our synthesis strategy relies on the grafting of the VOCl₃ molecular precursor onto various silica materials having different level of silanol density. To tune its surface chemistry, silica was treated at different temperatures (from 200 to 1000 °C) under high vacuum system (10⁻⁵ mbar) prior to the VOCl₃ grafting stage. Two kinds of typical absorption bands arising from ν(OH) stretching vibrations can be observed from the IR spectra of the SiO₂ treated at different temperatures (Figure 1a). The sharp classical band at around 3740 cm⁻¹ is ascribed to isolated silanols, whereas the broad band at 3500–3750 cm⁻¹ is attributed to silanols interacting between each other.^[10] The intensity of these two bands systematically decreases with increasing pretreatment temperature. Furthermore, when the SiO₂ treatment temperature was increased to 700 °C, the broad absorption band corresponding to the silanols interaction totally disappears, and only the sharp band from isolated silanols remains. Thus, the total amount of hydroxyl groups at the surface SiO₂ reduces gradually with the SiO₂ treatment temperature, and only one single type of silanol group is kept at the SiO₂ surface if it was calcined above 700 °C. Notably, the calcination temperature has a limited effect on the specific surface area of SiO₂ as shown in Table 1 (from 191 m²g⁻¹ at 200 °C down to 178 m²g⁻¹ at 1000 °C).

The SiO₂ treated at different temperatures subsequently reacts with the VOCl₃ in the H₂O-free system, which results in producing the VOCl_x/SiO₂ intermediate. The reaction between SiO₂ and VOCl₃ leads to a rapid and remarkable decrease of the sharp band at 3740 cm⁻¹ of the isolated silanol group in the IR spectra (Figure 1b). In most cases, this silanol group is completely consumed during the grafting procedure. On the contrary, the broad band attributed to the interacting silanols was kept nearly unchanged. Therefore, the isolated OH at the surface of SiO₂ can be considered as the active site for bonding the VOCl₃ species.

The VOCl_x/SiO₂ intermediate was then submitted to the calcination process at 600 °C in air, leading to the formation of VO_x/SiO₂ catalysts. Element analysis on the obtained VO_x/SiO₂ shows that the V content depends closely on the SiO₂ pretreatment temperature (Table 1). The VOCl₃ grafted onto the SiO₂ treated at higher temperature has lower V content. As revealed above, the amount of surface isolated OH groups, which are presumably the active center for grafting the VOCl₃ species, decreases with the treatment temperature. As a consequence, less VO_x is grafted at the surface of SiO₂ that was treated at higher temperature. Therefore, the V loading on the SiO₂ surface could be varied by changing the SiO₂ pretreatment temperature.

The BET surface area of the synthesized VO_x/SiO₂ sample decreases with the vanadium oxide loading (Table 1), which is consistent with the results of VO_x supported on MCM-41, MCM-48, and SBA-15 materials obtained by impregnation method.^[5a,11] The vanadium oxide species resulting from the air treatment, reacts with the OH group at the SiO₂ surface, thus a contraction of the SiO₂ structure may occur because of the

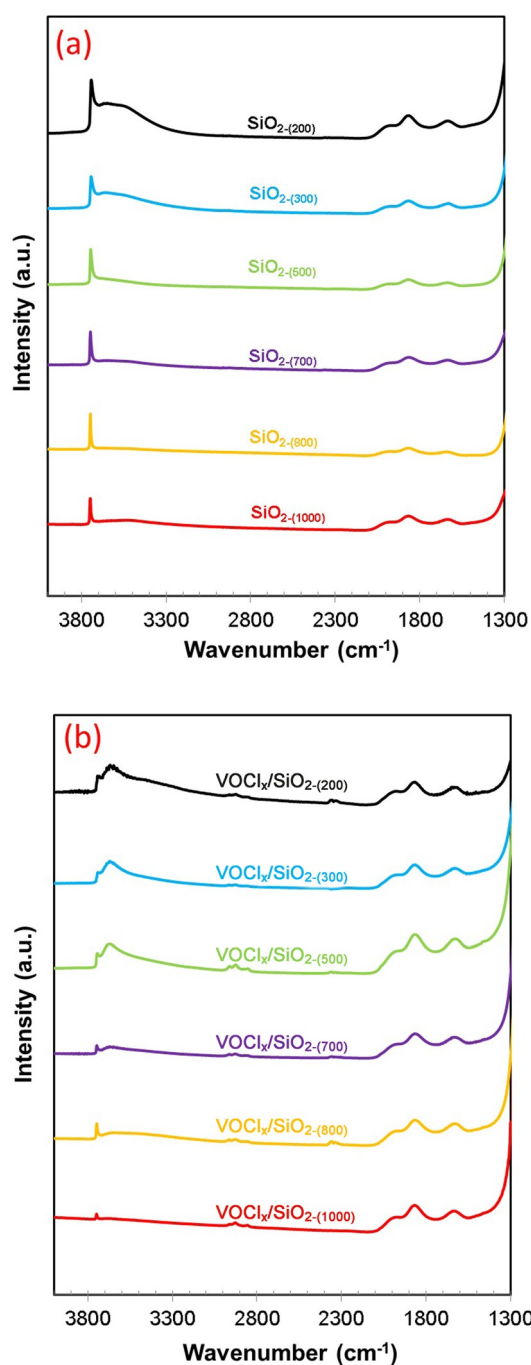


Figure 1. IR spectra of a) SiO₂ dehydroxylated at different temperatures under 10⁻⁵ mbar, b) VOCl₃ grafted onto various thermally treated SiO₂.

formation of new Si–O–V linkage at the surface of SiO₂.^[12] Therefore, the high loading of V on SiO₂ likely results in a decrease of the surface area by modification of the surface of silica.

The SEM images in Figure 2 show the morphology of the SiO₂ before and after grafting vanadium oxide at its surface. The SiO₂ is of spherical shape with a relatively uniform size of approximately 300 nm. Its morphology is well kept after vanadia loading at its surface. Except SiO₂, no other particle is observed on the prepared VO_x/SiO₂ sample, indicating that the VO_x exists as a high dispersed species at the surface of SiO₂.

Entry	V loading [%]	Surface area [m ² g ⁻¹] ^[a]	Surface area [m ² g ⁻¹] ^[b]
SiO ₂ -(200)	3.8	191	128
SiO ₂ -(300)	3.5	189	135
SiO ₂ -(500)	3.0	187	145
SiO ₂ -(700)	1.9	183	148
SiO ₂ -(800)	1.5	179	152
SiO ₂ -(1000)	1.0	178	155

[a] Surface area measured before grafting of VOCl₃. [b] Surface area of VO_x/SiO₂ catalysts.

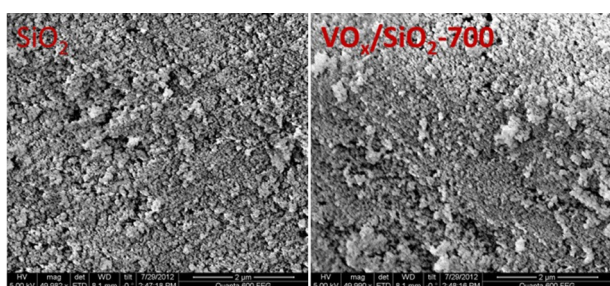


Figure 2. SEM images of SiO₂ and a typical VO_x/SiO₂-(700) catalyst. Scale bars = 2 µm.

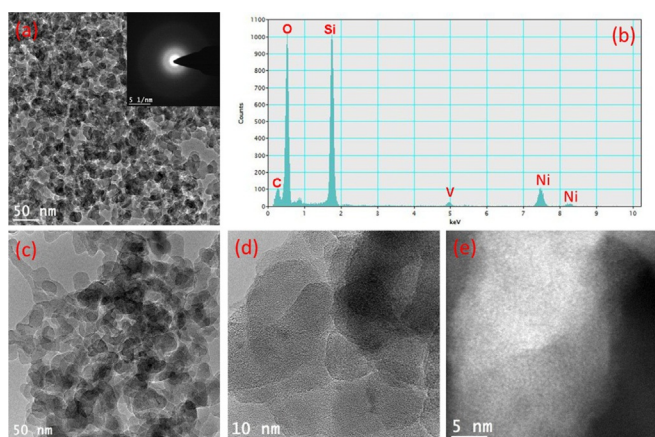


Figure 3. TEM and HAADF STEM of the VO_x/SiO₂-(700) sample: a) Low-magnification TEM image and selected-area electron diffraction pattern; b) energy-dispersive spectrometry (EDS) spectrum from the area in (a); c,d) high-magnification TEM images; and e) HAADF STEM image.

Further characterizations including TEM and STEM techniques (Figure 3) were also used to study the VO_x/SiO₂-(700) sample to provide more detailed information about its microstructure. The big particles observed in the SEM turned out to be the agglomerates of nanosized units having a size below 50 nm. The EDS spectrum from the area shown in Figure 3a reveals the existence of V, Si, and O elements in the sample, along with the Ni and C elements from the TEM grid. The selected-area electron diffraction (SAED) pattern in Figure 3a (inset) indicates that there is no crystalline structure in VO_x/

SiO₂-(700) sample. Only amorphous SiO₂ is observed in the high-resolution (HR) TEM image in Figure 3c, d, and there is no evident V₂O₅ crystal at the surface of SiO₂. High-angle annular dark-field (HAADF) STEM imaging technique in Figure 3e was further used to characterize this sample. This advanced technique is quite sensitive to the surface structure, and even small surface clusters can be detected.^[13] However, in Figure 3e no clear clusters were observable at the surface of VO_x/SiO₂-(700) sample. Therefore, from TEM and HAADF STEM characterizations, it can be concluded that the VO_x is highly dispersed at the SiO₂ surface without formation of crystalline structure.

The Raman spectroscopy is recognized to be a useful technique to study the dispersion and oligomeric state of surface VO_x species.^[14] It is well known that the structure of surface VO_x is quite sensitive to dehydroxylation conditions. The presence of H₂O can result in different levels of hydration process of the surface VO_x species, leading to the formation of a V₂O₅·nH₂O-like gel.^[5a,15] An in situ Raman spectroscopic measurement was thus performed in He gas flow at 500 °C. This testing condition is relatively close to the catalytic condition for propane ODH, and therefore the structure information of VO_x inferred from Raman spectroscopy will reflect to some extent its real structure in the catalytic process. As shown in Figure 4, a sharp peak located at 1040 cm⁻¹ is observed in all the samples, and this peak is generally attributed to the symmetric stretching mode of the V=O bond of the isolated tetrahedral VO₄ species at the surface of SiO₂. The shoulder peak at around 1060 cm⁻¹ is ascribed to ≡Si–O–V bond.^[11c,16] A broad band from 400 to 480 cm⁻¹ is attributed to the SiO₂ feature absorption.^[11c,16] Most importantly, no detectable band around 970 cm⁻¹ is observed in all the samples. This absorption band is usually ascribed to the formation of crystalline V₂O₅.^[5,11b,c] We can thus infer that the vanadium is highly dispersed at the surface of SiO₂ without formation of bulk V₂O₅ phase.

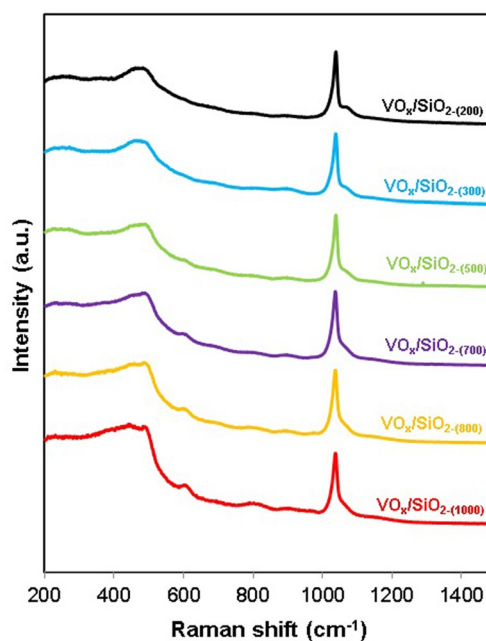


Figure 4. Raman spectra of VO_x/SiO₂ samples synthesized from grafting of VOCl₃ onto the SiO₂ treated at different temperature.

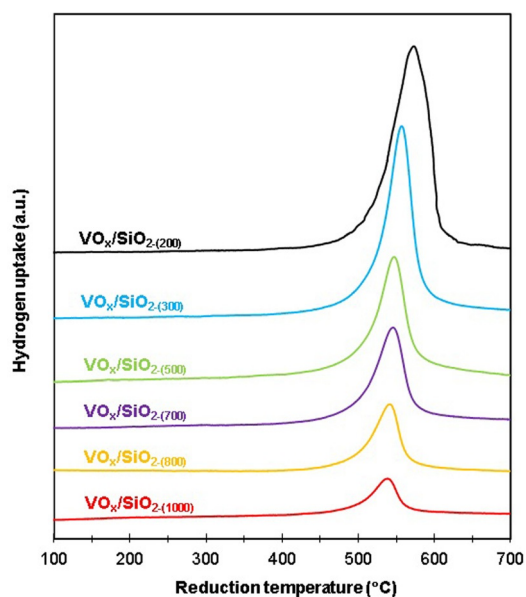


Figure 5. TPR profiles of VO_x/SiO_2 samples synthesized from grafting of VOCl_x onto the SiO_2 treated at different temperature.

The temperature-programmed reduction (TPR) profiles of VO_x/SiO_2 catalysts analyzed from room temperature to 700°C are shown in Figure 5. Only one sharp peak located from 530 to 570°C is detected in all the samples. This peak is attributed to the reduction of monomeric or low-oligomeric VO_x surface species.^[5a,11a,17] The intensities of these peaks decrease systematically with the SiO_2 pretreatment temperature, which is attributed to a lower V loading in the SiO_2 treated at higher temperature. Moreover, an increase of vanadium loading leads to a gradual shift of the reduction peak to high temperature. This observation is in agreement with TPR investigation on mesoporous-silica-supported VO_x catalysts.^[5b,11b] The progressive shift of the reduction peak to high temperature with the V loading is relevant to a gradual formation of a highly polymeric structure, which is less reducible in the TPR test. It should be noted that no reduction peak at approximately 590°C associated with the reduction of polymeric V^{5+} species in V_2O_5 -like structure is found in all the samples.^[5,11a,b] Therefore, the TPR characterization is consistent with Raman data, further confirming the high-level dispersion of VO_x at the SiO_2 surface.

Vanadium K-edge k^3 -weighted EXAFS signals for selected VO_x/SiO_2 samples with different V loadings and the corresponding Fourier transforms are shown in Figure 6 and extracted parameters given in Table 2. For all the samples, the first neighbor contribution is fitted with a total of four oxygen atoms separated in two scattering paths modeling

a vanadyl moiety and V–O single bonds. The coordination number of the short V=O double bond is in the range of $1.0\text{--}1.2 \pm 0.1$ at a distance of $1.58\text{--}1.62 \pm 0.01 \text{ \AA}$, and the coordination number of V–O single bond is in the range of $2.9\text{--}3.1 \pm 0.1$ at a distance of $1.84\text{--}1.89 \pm 0.02 \text{ \AA}$. Furthermore, the X-ray absorption near-edge spectroscopy (XANES) spectrum for each

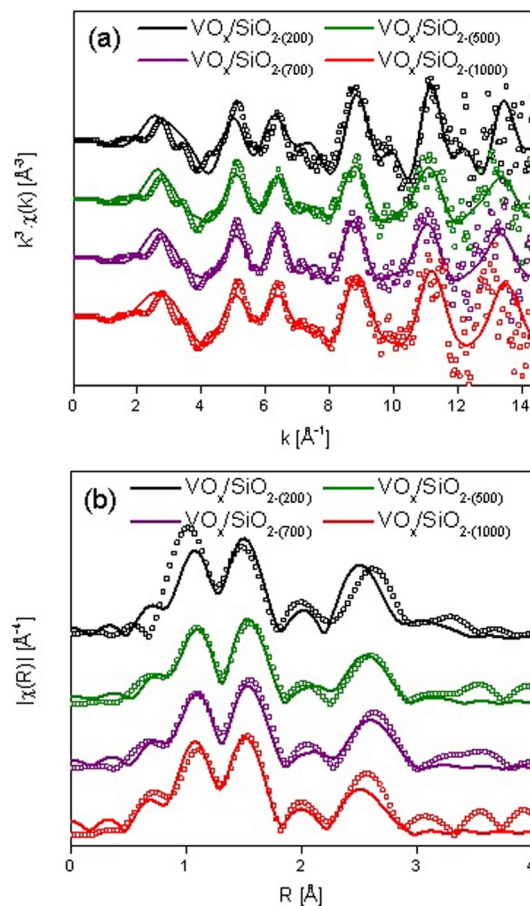


Figure 6. EXAFS $k^3\chi(k)$ functions (top) and Fourier transforms (bottom) for selected VO_x/SiO_2 samples with different V loadings. The solid lines are the experimental data and the dash lines are the fit results with a k range of $[2.3, 11.7] \text{ \AA}^{-1}$ and R range of $[0.5, 3.3] \text{ \AA}$.

Table 2. Parameters extracted from EXAFS fit of VO_x/SiO_2 samples. Italicized characters denote a fixed parameter.							
Sample	Shell	$N^{[a]}$	d [Å]	σ^2 [Å ²]	ΔE_0 [eV]	R -factor	
$\text{VO}_x/\text{SiO}_2-(200)$	V–O ₁	1.1 ± 0.1	1.58 ± 0.01	<i>0.0009</i>	-3.9 ± 1.5	0.065	
	V–O ₂	2.9 ± 0.1	1.85 ± 0.02	0.010 ± 0.002			
	V–V ^[b]	0.9 ± 0.2	3.02 ± 0.04	<i>0.002</i>			
$\text{VO}_x/\text{SiO}_2-(500)$	V–O ₁	0.9 ± 0.1	1.61 ± 0.01	<i>0.0009</i>	-0.7 ± 1.4	0.066	
	V–O ₂	3.1 ± 0.1	1.88 ± 0.02	0.012 ± 0.002			
	V–V ^[b]	0.6 ± 0.2	3.02 ± 0.04	<i>0.002</i>			
$\text{VO}_x/\text{SiO}_2-(700)$	V–O ₁	1.0 ± 0.1	1.62 ± 0.01	<i>0.0009</i>	-0.6 ± 1.3	0.057	
	V–O ₂	3.0 ± 0.1	1.89 ± 0.02	0.011 ± 0.001			
	V–V ^[b]	0.7 ± 0.1	3.03 ± 0.04	<i>0.002</i>			
$\text{VO}_x/\text{SiO}_2-(1000)$	V–O ₁	1.2 ± 0.1	1.59 ± 0.01	<i>0.0009</i>	-5.3 ± 2.0	0.071	
	V–O ₂	2.8 ± 0.1	1.84 ± 0.02	0.0085 ± 0.0016			
	V–V ^[b]	0.5 ± 0.2	3.00 ± 0.06	<i>0.002</i>			

[a] N refers to coordination number. [b] V–V scattering path is caused by a V–O–V arrangement.

compound depicted a very intense pre-edge located at 5470.5 eV (Figure S1). Intense transitions in the pre-edge region of K absorption edge for transition metals are known to occur if the local symmetry around the metal center does not include an inversion center.^[18] In this case, the hybridization of vanadium 3d with 4p states allows a large enhancement of the dipolar transitions in the pre-edge region. Thus, considering the presence of a vanadyl group and a total of four oxygen atoms in the first coordination sphere, the local symmetry around vanadium center would be consistent with a C_{3v} punctual group. It is also noteworthy to mention that the use of a V–Cl scattering path with a distance of 2.1 Å (Figure S2 and Table S1) did not improve any of the statistical agreement factors (R -factor and χ_r^2). Therefore, the chloride in $VOCl_x/SiO_2$ is totally removed after calcination in air. However, the fit was improved by including an additional V–V scattering path at 3.00–3.03 ± 0.04 Å. The latter V–V scattering path is ascribed to the condensation of two $[VO_4]$ units to create small oligomers at the surface of silica. Correlations between mean-square relative displacement and amplitude parameters prevented an accurate determination of the V–V coordination number. To compare materials at least relatively, the mean-square relative displacement was fixed to $0.2 \times 10^{-3} \text{ \AA}^2$ for all VO_x/SiO_2 samples.^[19] Doing so, the coordination number of V–V shell decreases from 0.9 ± 0.2 to 0.5 ± 0.2 as the pretreatment temperature of silica is increased from 200 °C to 1000 °C. The result is in accordance with Raman spectroscopy, which suggests that there is a certain amount of low-polymeric VO_x species at the surface of SiO_2 and the degree of oligomerization increases with V loading.

Based on the structural characterization results above, a configuration of the supported vanadium oxides is suggested and schematically depicted in Figure 7. As revealed from TEM, Raman spectroscopy, and H_2 TPR tests, no V_xO_y nanocrystallite is present in any of the samples. Further EXAFS analysis indicates that the vanadium oxide exists as low-polymeric VO_x species. The V–V coordination numbers for $[VO_4]$ monomer and $[V_2O_7]$ dimer are 0 and 1, respectively. Considering the experimental value obtained for the materials in the present study (between 0 and 1), we can describe the structure of the grafted vanadium oxide as a mixture of monomer and dimer. By using this simplified assumption, a general structure of vanadium oxide at the SiO_2 surface is shown in Figure 7. The configurations of vanadium oxides supported at SiO_2 , which is pretreated at three typical conditions: low (200 °C), moderate (700 °C), and high (1000 °C) temperatures, show a systematic

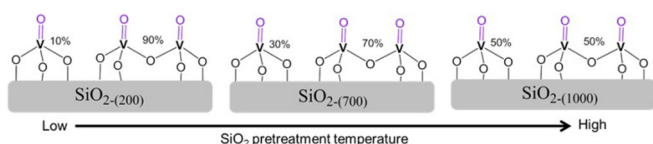


Figure 7. Schematic representation of molecular structure of vanadium oxides supported at SiO_2 pretreated at different temperature. The vanadium oxide groups at the SiO_2 surface are proposed to exist as $[VO_4]$ monomer and $[V_2O_7]$ dimer, and the proportion of dimers decreases with increasing SiO_2 calcination temperature.

decrease of the proportion of dimer from approximately 90% down to 50%. This is an important result as it proves that the tuning of the initial surface chemistry of silica has a strong impact on the final structure of grafted vanadium oxide.

Catalytic reaction

The catalytic performance of the SiO_2 -supported vanadium oxide catalyst was evaluated in the ODH reaction of propane in the temperature range 500 to 600 °C at atmospheric pressure. Propylene, carbon oxides including CO and CO_2 , methane, and ethylene are the gaseous products in the reaction. The liquid products are acrolein and acetaldehyde. The blank test on pure SiO_2 did not show propane conversion, whereas the VO_x/SiO_2 catalysts exhibits high performance in the propane ODH reaction.

The six VO_x/SiO_2 catalysts show different level of activity for the propane ODH reaction (Figure 8a). High activities are observed in these catalysts at 600 °C, and the corresponding propane conversions vary from 25% to 55%. Among these catalysts, the VO_x supported on $SiO_{2-(200)}$ exhibits the highest propane conversion. With the increase of the silica treatment temperature, the catalyst activity slowly decreases. The lowest propane conversion is observed with $VO_x/SiO_{2-(1000)}$ catalyst. As described above, the VO_x loading is related to the SiO_2 pre-

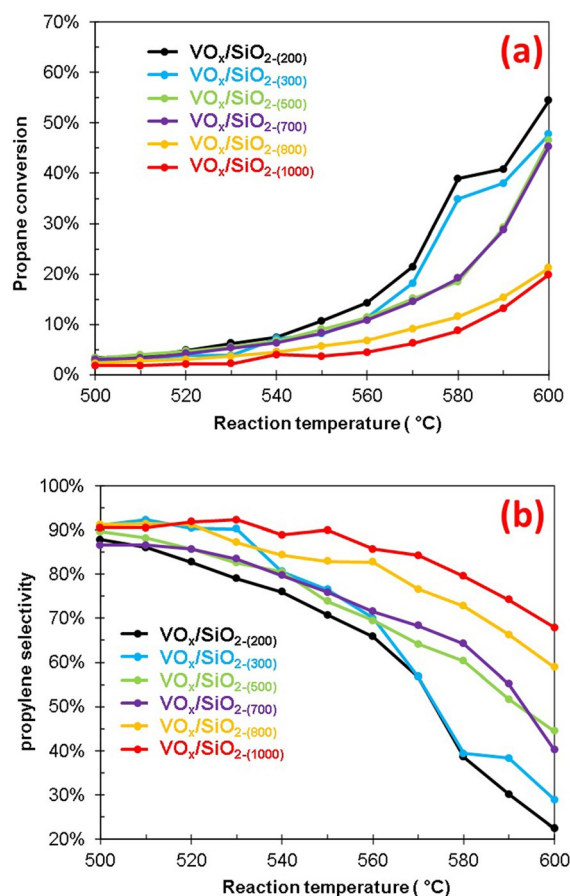


Figure 8. a) Propane conversion and b) propylene selectivity on the different VO_x/SiO_2 catalysts in propane ODH reaction.

treatment temperature, and the SiO₂ calcined at lower temperature results in higher content of VO_x at its surface. Therefore, more active species is located at the surface of SiO₂ treated at low temperature. Accordingly, high propane conversion is achieved on the VO_x supported on the SiO₂ treated at low temperature.

In contrast to propane conversion, the propylene selectivity is reversely correlated with the V loading in SiO₂ (Figure 8b). Overall, the propylene selectivity increases systematically with the decrease of V loading, and the VO_x/SiO₂₋₍₁₀₀₀₎ catalyst shows the highest propylene selectivity. In addition, it is evident that the propylene selectivity decreases dramatically with the reaction temperature, which is a result of the deep oxidation of propane at high temperature. Appreciable propylene selectivity is achieved in the VO_x/SiO₂₋₍₁₀₀₀₎ catalyst. In this catalyst, high propylene selectivity of approximately 90% at 500 °C is obtained, and a selectivity of 68% still remains at 600 °C.

The propylene selectivity is related not only to the reaction temperature but also to the propane conversion. To obtain a better understanding of the reaction network, the variation of the propylene selectivity with the propane conversion at 550 °C was analyzed by changing the contact time (0.025 gsmL⁻¹ < W/F < 0.15 gsmL⁻¹) in the reaction (Figure 9). Clearly, the selectivity to propylene decreases significantly with the propane conversion in all the vanadium oxide catalysts, which suggests the overoxidation of propylene into CO_x.^[5, 11b, 20] The selectivity to propylene is close to 100% if the propane conversion is extrapolated to zero. Therefore, all the byproducts are mainly produced directly from the overoxidation of propylene, indicating a consecutive reaction network in propane ODH reaction. On the other hand, the propylene selectivity is negatively relevant to the V loading, and the VO_x/SiO₂₋₍₁₀₀₀₎ catalyst shows the highest selectivity. Low density of VO_x at the surface SiO₂₋₍₁₀₀₀₎ results in highly dispersed vanadia species at SiO₂ surface. Low polymeric VO_x species is therefore the predominant structure at the surface SiO₂₋₍₁₀₀₀₎. The highly dispersed VO_x species, such as isolated VO_x is believed to be more selective for the formation of propylene.

The influence of O₂/C₃H₈ ratio on the selectivity was studied at 550 °C on the VO_x/SiO₂₋₍₁₀₀₀₎ catalyst. The propane concentra-

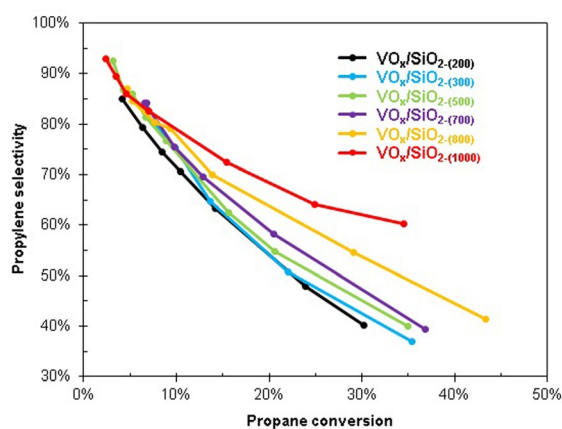


Figure 9. Propane conversion versus propylene selectivity on different VO_x/SiO₂ in propane ODH reaction.

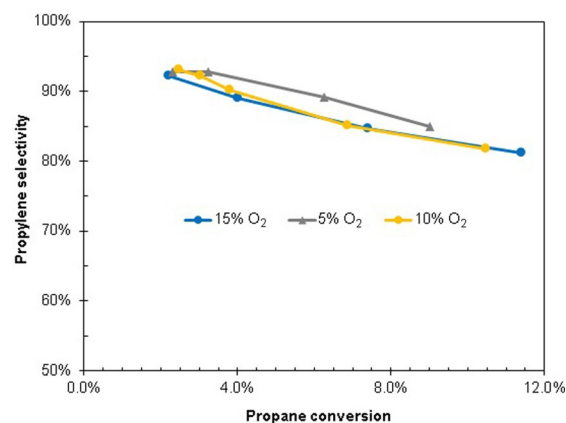


Figure 10. Effect of O₂/C₃H₈ ratio on the propylene selectivity in propane ODH reaction over VO_x/SiO₂₋₍₁₀₀₀₎ catalyst at 550 °C.

tion in the feed was kept constant (10%), and the O₂ concentration in the feed was varied from 5% to 15% to obtain different O₂/C₃H₈ ratios. The O₂/C₃H₈ ratio has a limited effect on the propylene selectivity in the propane ODH reaction (Figure 10). With the same level of propane conversion, the propylene selectivity does not change much with the O₂/C₃H₈ ratios. Therefore, the propylene formation rate is independent on the O₂ partial pressure, and the variation of O₂/C₃H₈ ratio does not change the propylene selectivity. As confirmed in a previous study, the reaction order in oxygen is zero in the propene combustion reaction,^[21] and the change of O₂/C₃H₈ ratio thus has no substantial effect on the propylene selectivity.

As shown above, the VO_x/SiO₂₋₍₁₀₀₀₎ catalyst exhibits the highest selectivity to propylene, which could be a reasonably good catalyst for the production of propylene from propane. The stability of the catalyst with time is an important parameter for its practical application. The VO_x/SiO₂₋₍₁₀₀₀₎ catalyst was further investigated at 580 °C with time-on-stream of 72 h. As shown in Figure 11, the initial propane conversion (≈31%) is quite stable in the long-term test, and does not change with time on stream. The calculated TOF_{propane} value at this reaction condition is 2.59 min⁻¹, which is close to the results in the previous reports.^[4–9] More importantly, the selectivities to all the products including propylene, ethylene, CO, CO₂, acetaldehyde, and acrolein are substantially maintained in 72 h catalytic reaction. The propylene selectivity of 60% is well kept, which corresponds to the propylene yield of 18%. No activity loss in VO_x/SiO₂₋₍₁₀₀₀₎ catalyst indicates that the intrinsic active site (highly dispersed vanadium oxide) in the catalyst is very stable at such high-temperature reaction, and it is resistant to this harsh reaction condition. Therefore, the VO_x/SiO₂₋₍₁₀₀₀₎ material could be a fairly good candidate for propane ODH in the practical industrial application thanks to its high stability in the reaction.

The chemistry of the silanol group at the SiO₂ surface strongly relies on its treatment temperature under the high-vacuum technique. Isolated, geminal, and vicinal silanols are the typical OH group at the SiO₂ surface. SiO₂ treated at low temperatures from 200 to 500 °C, has high density of OH group with various kinds of silanol group. By contrast, if the

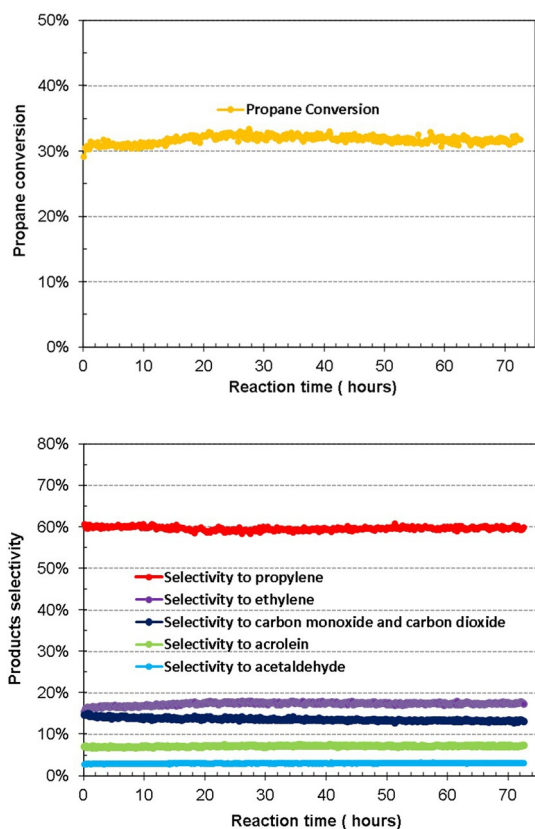


Figure 11. Propane conversion (top) and product selectivities (bottom) with time on stream over $\text{VO}_x/\text{SiO}_{2-(1000)}$ catalyst for propane ODH reaction at 580°C .

SiO_2 was treated above 700°C , only isolated OH groups exist at the surface of SiO_2 . The VOCl_3 reacting with these isolated OH groups is beneficial for getting highly dispersed vanadium oxide species at silica surface, because the low density of OH group can prevent the formation of highly polymeric vanadia species. In such a case, highly dispersed vanadium oxide forms at the surface of SiO_2 that was treated at high temperature. The catalyst with low V loading, such as $\text{VO}_x/\text{SiO}_{2-(1000)}$ has shown high performance in propane oxidative dehydrogenation reaction, because the highly dispersed VO_x species is beneficial for the formation of propylene.

Conclusions

A series of VO_x/SiO_2 catalysts have been prepared by grafting VOCl_3 at the surface of SiO_2 , which was dehydrated before at different temperatures under vacuum. The SiO_2 pretreatment temperature affects the density and structure of silanol group at the surface of SiO_2 . The nature of silanol group has a significant impact on the dispersion of VO_x at the surface of SiO_2 . The SiO_2 treated at high temperature results in low loading and high dispersion of VO_x at the SiO_2 surface, which produces efficient VO_x/SiO_2 catalysts for the propane oxidative dehydrogenation reaction. The prepared $\text{VO}_x/\text{SiO}_{2-(1000)}$ catalyst exhibits the highest selectivity to propylene in the reaction and achieves 18% propylene yield in this reaction. Moreover, the activity and selectivity achieved on $\text{VO}_x/\text{SiO}_{2-(1000)}$ catalyst are quite

stable in 72 h time-on-stream reaction. Thus, these VO_x/SiO_2 materials prepared by the grafting method could be the potential catalyst for the production of propylene from propane oxidative dehydrogenation process.

Experimental Section

Catalyst preparation

The silica used in the study was nonporous Degussa Aerosil-200, with a BET surface area $\approx 200\text{ m}^2\text{g}^{-1}$. The commercial available VOCl_3 (99%, Sigma Aldrich) was distilled under vacuum at RT before grafting. The silica was dehydroxylated by calcination under vacuum (10^{-5} mbar) for 8 h at 200, 300, 500, 700, 800, and 1000°C , respectively. The dehydroxylated SiO_2 was then transferred into a hexane solution of VOCl_3 in the Schlenk tube. The resulting mixture was kept on stirring for 4 h at RT. The yellow powder was separated from solution by filtration in the glove box, and afterwards the isolated powder washed with hexane several time to remove any physical adsorbed VOCl_3 . Finally, the obtained powder was calcined in the air at 600°C for 4 h to obtain $\text{VO}_x/\text{SiO}_{2-(T)}$ catalyst. The synthesized catalysts are denoted as $\text{VO}_x/\text{SiO}_{2-(T)}$, where T is the silica dehydrogenation temperature.

Characterization

N_2 adsorption/desorption isotherms were acquired from a Micromeritics ASAP2420, and the samples were degassed for 2 h at 500°C before the measurement. The surface areas of the samples were calculated by multipoint BET analysis method. The SEM of the catalyst was taken from an FEI Quanta 600 FEG environmental scanning electron microscope (ESEM). The TEM and HAADF STEM analyses were conducted on aberration-corrected FEI Titan instrument. Samples were dispersed in ethanol with the help of ultrasound treatment, and then supported onto a 200 mesh carbon-coated nickel grid before TEM measurement. In situ Raman spectra were recorded on a Horiba Yvon LabRAM Aramis with a CCD-camera as a detector using a $100\times$ objective, a 600 grmm^{-1} grating, a $100\text{ }\mu\text{m}$ hole, a $100\text{ }\mu\text{m}$ slit, a D1 filter, and a 473 nm cobalt laser. The sample was pressed into thin pellet and then loaded in an in situ chamber. All spectra were recorded at 500°C in He gas flow. TPR measurements were performed on an Altamira Instrument equipped with a TCD detector. The catalyst powder (10 mg) was placed in a U-shaped quartz reactor and pretreated in flowing Ar (30 mL min^{-1}) for 0.5 h at 350°C , followed by cooling to RT. The temperature was then raised from RT to 700°C at a rate of $10^\circ\text{C min}^{-1}$ in a 5% H_2/Ar flow (30 mL min^{-1}).

X-ray absorption spectroscopy (XAS) experiments were performed on the CRG-FAME beamline (BM30B), at the European Synchrotron Radiation Facility in Grenoble. Spectra were recorded either in fluorescence (VO_x/SiO_2) or in transmission ($\text{V(=O)(O}i\text{Pr)}_3$ reference) modes at the V/K-edge (5.465 keV). XAS data were analyzed using the HORAE package, a graphical interface to the AUTOBK and IFFFIT code and Cherokee software (for the extraction of the EXAFS signal).^[22] XANES and EXAFS spectra were obtained after performing standard procedures for pre-edge subtraction, normalization, polynomial removal and wave vector conversion. The extracted EXAFS signal was fitted in $k^3\chi(k)$ without any additional filtering. Fitting was conducted in k -space between 2.1 and $12.3\text{ }\text{\AA}^{-1}$ for $\text{V(=O)(O}i\text{Pr)}_3$ and, between 2.0 and $12.5\text{ }\text{\AA}^{-1}$ for VO_x/SiO_2 . During the fitting procedure, a restriction on the number of fitted parameters was taken into account: Δk and ΔR allowed at least 15 param-

eters and 12 parameters were used at most to describe different paths. Determination of the energy level (E_0) was performed at the first inflection point of the edge. For each atomic shell, the following structural parameters were adjusted: coordination number (N), bond length (R), and the so-called Debye–Waller factor through the mean-square relative displacement (σ^2) of the considered bond length. The amplitude factor (S_0^2) was fitted to the EXAFS spectrum obtained for $V(=O)(O_iPr)_3$. To do so, a molecular model of $V(=O)(O_iPr)_3$ was built and optimized at the UFF^[23] level with the Avogadro molecular builder and visualization tool.^[24] Then the geometry of the whole structure was fully optimized at the DFT level from Gaussian09^[25] code using the MO6^[26] functional and TZVP^[27] basis set for all the atoms except for the vanadium atom to which we described the electronic structure of s and p core electrons from the Stuttgart/Dresden^[28] effective core potential. The resulting atomic coordinates were used as an input to calculate the theoretical phases, amplitudes and electron free mean path with the FEFF6 code^[29] implemented in IFFEFIT programs suite. S_0^2 for $V(=O)(O_iPr)_3$ was then found equal to 0.87.

Catalytic tests

Catalytic propane ODH was performed on a micropilot (from PID Eng&Tech) equipped with a quartz glass reactor at atmospheric pressure. The catalyst powder (25 mg) was placed in the reactor supported by quartz glass wool. The effect of temperature on the activity and selectivity was measured from 500 to 600 °C, and the gas feed composed of 10% C_3H_8 and 10% O_2 in He was introduced through the catalytic bed at a total flow rate of 30 mL/minute. The propane conversion versus propylene selectivity was determined at 550 °C, and the total flow rate (10% C_3H_8 and 10% O_2) was changed from 10 mL/min to 60 mL/min. The stability test was evaluated at 580 °C with total flow rate of 10 mL/min (10% C_3H_8 and 10% O_2). The reaction products were analyzed with on-line Varian 490 micro-GC equipped with a TCD detector and four columns: a MolSieve 5 Å column to quantify O_2 and CO , a poraPLOT Q column to quantify CO_2 , C_2H_4 as well as C_2H_6 , an alumina column to quantify C_3H_8 as well as C_3H_6 . Propane conversion and selectivity to propylene were calculated on a carbon basis. Carbon mass balance was superior to 98% in all cases.

Keywords: alkanes · alkenes · dehydrogenation · silicates · vanadium

- a) M. M. Bhasin, J. H. McCain, B. V. Vora, T. Imai, P. R. Pujadó, *Appl. Catal. A* **2001**, *221*, 397–419; b) F. Cavani, N. Ballarini, A. Cericola, *Catal. Today* **2007**, *127*, 113–131.
- a) A. Corma, F. Melo, L. Sauvanaud, F. J. Ortega, *Appl. Catal. A* **2004**, *265*, 195–206; b) Q. Shao, P. Wang, H. Tian, R. Yao, Y. Sun, J. Long, *Catal. Today* **2009**, *147*, S347–S351.
- a) Z. Bai, P. Li, L. Liu, G. Xiong, *ChemCatChem* **2012**, *4*, 260–264; b) Y. V. Kolen'ko, W. Zhang, R. N. d'Alnoncourt, F. Girgsdies, T. W. Hansen, T. Wolfram, R. Schlögl, A. Trunschke, *ChemCatChem* **2011**, *3*, 1597–1606; c) X. Sun, R. Wang, B. Zhang, R. Huang, X. Huang, D. S. Su, T. Chen, C. Miao, W. Yang, *ChemCatChem* **2014**, *6*, 2270–2275; d) S. R. G. Carrazán, C. Peres, J. P. Bernard, M. Ruwet, R. Ruiz, B. Delmon, *J. Catal.* **1996**, *158*, 452–476; e) K. Chalupka, C. Thomas, Y. Millot, F. Averseng, S. Dzwigaj, *J. Catal.* **2013**, *305*, 46–55.
- a) C. A. Carrero, R. Schloegl, I. E. Wachs, R. Schomaecker, *ACS Catal.* **2014**, *4*, 3357–3380; b) R. Grabowski, *Catal. Rev. Sci. Eng.* **2006**, *48*, 199–268; c) H. H. Kung, *Adv. Catal.* **1994**, *40*, 1–38.
- a) Y.-M. Liu, Y. Cao, N. Yi, W.-L. Feng, W.-L. Dai, S.-R. Yan, H.-Y. He, K.-N. Fan, *J. Catal.* **2004**, *224*, 417–428; b) Y.-M. Liu, W.-L. Feng, T.-C. Li, H.-Y. He, W.-L. Dai, W. Huang, Y. Cao, K.-N. Fan, *J. Catal.* **2006**, *239*, 125–136.
- A. Comite, A. Sorrentino, G. Capannelli, M. Di Serio, R. Tesser, E. Santacesaria, *J. Mol. Catal. A* **2003**, *198*, 151–165.
- a) J. L. Male, H. G. Niessen, A. T. Bell, T. Don Tilley, *J. Catal.* **2000**, *194*, 431–444; b) C. Pak, A. T. Bell, T. D. Tilley, *J. Catal.* **2002**, *206*, 49–59.
- J. Keränen, P. Carniti, A. Gervasini, E. Iiskola, A. Auroux, L. Niinistö, *Catal. Today* **2004**, *91–92*, 67–71.
- B. Schimmoeller, S. E. Pratsinis, A. Baiker, *ChemCatChem* **2011**, *3*, 1234–1256.
- a) L. T. Zhuravlev, *Colloids Surf. A* **2000**, *173*, 1–38; b) X. Rozanska, F. Delbecq, P. Sautet, *Phys. Chem. Chem. Phys.* **2010**, *12*, 14930–14940; c) L. Lefort, M. Chabanas, O. Maury, D. Meunier, C. Copéret, J. Thivolle-Cazat, J.-M. Basset, *J. Organomet. Chem.* **2000**, *593–594*, 96–100.
- a) H. Berndt, A. Martin, A. Brückner, E. Schreier, D. Müller, H. Kosslick, G. U. Wolf, B. Lücke, *J. Catal.* **2000**, *191*, 384–400; b) B. Solsona, T. Blasco, J. M. López Nieto, M. L. Peña, F. Rey, A. Vidal-Moya, *J. Catal.* **2001**, *203*, 443–452; c) C. Hess, G. Tzolova-Müller, R. Herbert, *J. Phys. Chem. C* **2007**, *111*, 9471–9479.
- M. Morey, A. Davidson, H. Eckert, G. Stucky, *Chem. Mater.* **1996**, *8*, 486–492.
- a) W. Zhou, E. I. Ross-Medgaarden, W. V. Knowles, M. S. Wong, I. E. Wachs, C. J. Kiely, *Nat. Chem.* **2009**, *1*, 722–728; b) B. Qiao, A. Wang, X. Yang, L. F. Allard, Z. Jiang, Y. Cui, J. Liu, J. Li, T. Zhang, *Nat. Chem.* **2011**, *3*, 634–641.
- Y. T. Chua, P. C. Stair, I. E. Wachs, *J. Phys. Chem. B* **2001**, *105*, 8600–8606.
- S. Xie, E. Iglesia, A. T. Bell, *Langmuir* **2000**, *16*, 7162–7167.
- X. Gao, S. R. Bare, B. M. Weckhuysen, I. E. Wachs, *J. Phys. Chem. B* **1998**, *102*, 10842–10852.
- F. Arena, N. Giordano, A. Parmaliana, *J. Catal.* **1997**, *167*, 66–76.
- a) F. de Groot, G. Vankó, P. Glatzel, *J. Phys. Condens. Matter* **2009**, *21*, 104207; b) D. Cabaret, A. Bordage, A. Juhin, M. Arfaoui, E. Gaudry, *Phys. Chem. Chem. Phys.* **2010**, *12*, 5619–5633.
- A. L. Hector, W. Levason, A. J. Middleton, G. Reid, M. Webster, *Eur. J. Inorg. Chem.* **2007**, 3655–3662.
- a) B. Frank, M. Morassutto, R. Schomäcker, R. Schlögl, D. S. Su, *ChemCatChem* **2010**, *2*, 644–648; b) I. Rossetti, L. Fabbrini, N. Ballarini, C. Oliva, F. Cavani, A. Cericola, B. Bonelli, M. Piumetti, E. Garrone, H. Dyrbeck, E. A. Blekkan, L. Forni, *J. Catal.* **2008**, *256*, 45–61.
- A. Dinse, S. Khennache, B. Frank, C. Hess, R. Herbert, S. Wrabetz, R. Schlögl, R. Schomäcker, *J. Mol. Catal. A* **2009**, *307*, 43–50.
- a) B. Ravel, M. Newville, *J. Synchrotron Radiat.* **2005**, *12*, 537–541; b) M. Alain, M. Jacques, M.-B. Diane, P. Karine, *J. Phys. Conf. Ser.* **2009**, *190*, 012034–012035.
- A. K. Rappe, C. J. Casewit, K. S. Colwell, W. A. Goddard, W. M. Skiff, *J. Am. Chem. Soc.* **1992**, *114*, 10024–10035.
- M. Hanwell, D. Curtis, D. Lonie, T. Vandermeersch, E. Zurek, G. Hutchison, *J. Cheminf.* **2012**, *4*, 17.
- Gaussian 09, Revision D.01, M. J. Frisch, G. W. Trucks, H. B. Schlegel, G. E. Scuseria, M. A. Robb, J. R. Cheeseman, G. Scalmani, V. Barone, B. Menonucci, G. A. Petersson, H. Nakatsuji, M. Caricato, X. Li, H. P. Hratchian, A. F. Izmaylov, J. Bloino, G. Zheng, J. L. Sonnenberg, M. Hada, M. Ehara, K. Toyota, R. Fukuda, J. Hasegawa, M. Ishida, T. Nakajima, Y. Honda, O. Kitao, H. Nakai, T. Vreven, J. A. Montgomery, Jr., J. E. Peralta, F. Ogliaro, M. Bearpark, J. J. Heyd, E. Brothers, K. N. Kudin, V. N. Staroverov, R. Kobayashi, J. Normand, K. Raghavachari, A. Rendell, J. C. Burant, S. S. Iyengar, J. Tomasi, M. Cossi, N. Rega, J. M. Millam, M. Klene, J. E. Knox, J. B. Cross, V. Bakken, C. Adamo, J. Jaramillo, R. Gomperts, R. E. Stratmann, O. Yazyev, A. J. Austin, R. Cammi, C. Pomelli, J. W. Ochterski, R. L. Martin, K. Morokuma, V. G. Zakrzewski, G. A. Voth, P. Salvador, J. J. Dannenberg, S. Dapprich, A. D. Daniels, Ö. Farkas, J. B. Foresman, J. V. Ortiz, J. Cio-slowski, D. J. Fox, Gaussian, Inc., Wallingford CT, **2009**.
- Y. Zhao, D. Truhlar, *Theor. Chem. Acc.* **2008**, *120*, 215–241.
- A. Schäfer, C. Huber, R. Ahlrichs, *J. Chem. Phys.* **1994**, *100*, 5829–5835.
- D. Andrae, U. Häußermann, M. Dolg, H. Stoll, H. Preuß, *Theor. Chim. Acta* **1990**, *77*, 123–141.
- S. I. Zabinsky, J. J. Rehr, A. Ankudinov, R. C. Albers, M. J. Eller, *Phys. Rev. B* **1995**, *52*, 2995–300.

Received: May 30, 2015

Published online on September 7, 2015